Quasi-one-dimensional solutions and their interaction with two-dimensional dissipative solitons

Orazio Descalzi[1,2,*] and Helmut R. Brand[2]

[1]*Complex Systems Group, Facultad de Ingeniería y Ciencias Aplicadas, Universidad de los Andes, Avenida San Carlos de Apoquindo 2200, Santiago, Chile*

[2]*Department of Physics, University of Bayreuth, 95440 Bayreuth, Germany*

(Received 25 June 2012; revised manuscript received 6 January 2013; published 26 February 2013)

We describe the stable existence of quasi-one-dimensional solutions of the two-dimensional cubic-quintic complex Ginzburg-Landau equation for a large range of the bifurcation parameter. By quasi-one-dimensional (quasi-1D) in the present context, we mean solutions of fixed shape in one spatial dimension that are simultaneously fully extended and space filling in a second direction. This class of stable solutions arises for parameter values for which simultaneously other classes of solutions are at least locally stable: the zero solution, 2D fixed shape dissipative solitons, or 2D azimuthally symmetric or asymmetric exploding dissipative solitons. We show that quasi-1D solutions can form stable compound states with 2D stationary dissipative solitons or with azimuthally symmetric exploding dissipative solitons. In addition, we find stable breathing quasi-1D solutions near the transition to collapse. The analogy of several features of the work presented here to recent experimental results on convection by Miranda and Burguete [Phys. Rev. E **78**, 046305 (2008); Phys. Rev. E **79**, 046201 (2009)] is elucidated.

DOI: 10.1103/PhysRevE.87.022915 PACS number(s): 82.40.Bj, 42.65.Sf, 47.20.Ky, 05.70.Ln

I. INTRODUCTION

The stable existence of quasi-one-dimensional (quasi-1D) solutions was described first in the field of nonlinear optics; specifically, for a laser with a saturable absorber an envelope equation with complex coefficients was derived and shown to allow for the stable existence of quasi-1D localized solutions of fixed shape for fixed parameter values in the equation [1]. Later on, the stable existence of quasi-1D solutions was discussed for the cubic-quintic Swift-Hohenberg equation with real coefficients [2], which is well known to allow for the existence of localized solutions of many different lengths due to the trapping mechanism [2]. This early work [1,2] was generalized later to other physical systems as well as to other equations [3–5].

Here we investigate the cubic-quintic complex Ginzburg-Landau equation, which is a prototype envelope equation associated with the vicinity of a weakly inverted bifurcation to traveling waves. We find a large range of stable existence of stationary quasi-1D solutions and verify this feature by showing their stability to noisy perturbations. In addition, we find stable breathing quasi-1D solutions near the transition from stationary quasi-1D solutions to collapse (zero amplitude).

The experimental results most closely related to our present work are clearly those by Miranda and Burguete [6,7]. They have demonstrated recently for a convective system a route to spatiotemporal chaos in an extended one-dimensional array of convective oscillators. Their localized stationary mode is the analog of our stationary quasi-1D pattern and their ST/ALT mode for the oscillatory domains (compare Figs. 2 of Refs. [6,7]) is the analog of our breathing quasi-1D solution. In making this comparison one must keep in mind that we are looking at the patterns in the framework of an envelope equation for which one has split off the rapid spatial variation of the spatial profile of the rolls.

The present work is part of the larger field of spatially localized solutions in dissipative systems. Such stable localized objects have been investigated for a number of dissipative systems [1,8–29], both experimentally [9,12–14,20,23,25–27], and theoretically [1,8,10,11,15–19,21,22,24,28,29], in systems as diverse as surface reactions [14], binary fluid convection [12,13], sheared electroconvection in liquid crystals [27], and nonlinear optics [9,23,26] for about 20 years. These stable localized solutions, also called dissipative solitons, exist stably not only in one but also in two spatial dimensions [1,10,14,15,17–20,22–28], setting them apart from systems without dissipation. This is due to the fact that solitons in nondissipative systems are in most cases unstable to perturbations in a second direction [30].

Outstanding among the recent developments in the field are exploding dissipative solitons, which were pioneered by Akhmediev *et al.* for anomalous linear dispersion in the cubic-quintic complex Ginzburg-Landau equation [8], and which have been further studied experimentally [9] and theoretically [31–35] in one spatial dimension, incorporating most recently the influence of a small amount of noise, which produces qualitative changes [36]. It has also been shown that a number of temporally regular localized solutions arise when increasing the bifurcation parameter μ, the distance from linear onset, towards the regime for which explosive dissipative solitons are found [34,35].

Depending on the parameter values, quasi-1D states have overlap in their regime of stable existence with several other types of 2D dissipative solitons, namely, stationary 2D radially symmetric localized solutions, azimuthally symmetric exploding dissipative solitons, and asymmetric exploding dissipative solitons. Thus the present investigation of quasi-1D states ties in closely with recent work on explosive dissipative solitons in the two-dimensional cubic-quintic complex Ginzburg-Landau equation with positive linear dispersion, which have been studied as a function of the bifurcation parameter μ and the cubic nonlinear refractive index β_i [37]. As a main result a transition between azimuthally symmetric and asymmetric

*Email address: odescalzi@miuandes.cl

exploding dissipative solitons was found [37], which is not even known in one-dimensional systems.

Here we describe the observation of two classes of stable compound states; one is composed of a quasi-1D state and a stationary radially symmetric 2D dissipative soliton while the other consists of a combination of a quasi-1D state with a 2D azimuthally symmetric exploding dissipative soliton. We find that 2D asymmetric exploding dissipative solitons are always wiped out in collisions in the long time limit as soon as a stable quasi-1D localized solution is formed. Two quasi-1D localized solutions when brought sufficiently close to each other lead to one quasi-1D localized solution in a process reminiscent of the partial annihilation of pulses [29].

II. THE MODEL

The two-dimensional cubic-quintic complex Ginzburg-Landau equation reads

$$\partial_t A = \mu A + (\beta_r + i\beta_i)|A|^2 A + (\gamma_r + i\gamma_i)|A|^4 A + (D_r + iD_i)\nabla^2 A, \quad (1)$$

where $A(x,y;t)$ is a complex field, β_r is positive, and γ_r is negative in order to guarantee that the bifurcation is subcritical, but saturates to quintic order. The diffusion coefficient D_r and the linear dispersion D_i are positive. Equation (1) is an equation for the envelope of the linear modes near the onset of a subcritical oscillatory instability.

In nonlinear optics, an equation similar in structure can be derived:

$$i\psi_z + \frac{D}{2}\nabla_\perp^2\psi + |\psi|^2\psi + \nu|\psi|^4\psi = i\delta\psi + i\sigma|\psi|^2\psi + i\beta\nabla_\perp^2\psi + i\mu|\psi|^4\psi. \quad (2)$$

Here $\psi(x,y,z)$ is the normalized envelope of the propagating electrical field, ${\nabla_\perp}^2 = \partial_x^2 + \partial_y^2$ is the two-dimensional transverse Laplacian, z is the propagation distance, and D is the diffraction coefficient. Since the spatially localized structures are the result of a balance between gain and loss of the media, as well as the balance between diffraction and nonlinearities, δ stands for linear losses, σ and μ are the cubic and quintic nonlinear gain and absorption, respectively, ν is the saturation coefficient of the Kerr nonlinearity, and β stands for spectral filtering in the medium.

For the simulation of Eq. (1) we use two independent numerical methods: (I) explicit fourth-order Runge-Kutta finite differencing with a grid of 250×250 points in (x,y) along a grid spacing of $dx = dy = 0.2$ (corresponding to a box size 50×50) and a time step $dt = 0.01$; (II) a pseudospectral split-step scheme using a fourth-order Runge-Kutta method to integrate the nonlinear part of Eq. (1) using a square box of size 50×50, 256×256 points, $dx = dy = \frac{L}{256}$ with $L = 50$, and $dt = 0.01$. To accelerate our codes we used the PYCUDA extension [38]. The stability of the solutions has been tested by introducing a small amount of noise and waiting long enough to avoid transients (in some cases $T \sim 10^6$).

In our numerical simulations we keep all parameters fixed except for μ, the distance from linear onset, and β_i, the cubic nonlinear refractive index. The parameter values are $\beta_r = 1$, $\gamma_r = -0.1$, $\gamma_i = -0.6$, $D_r = 0.125$, and $D_i = 0.5$. Different solutions arise as a function of the control parameter

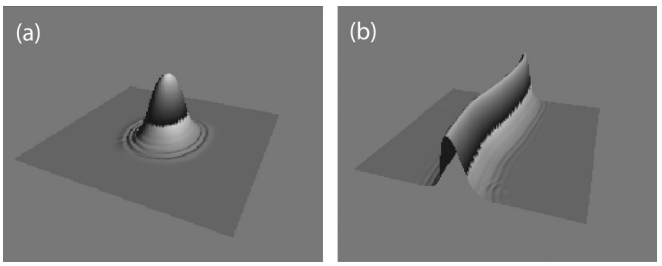

FIG. 1. (a) $|A(x,y)|$ for a generic localized initial condition (LIC); (b) $|A(x,y)|$ for a generic nonlocalized initial condition (NLIC).

μ, β_i, and the initial conditions. Qualitatively we use two classes of initial conditions: localized initial conditions (LICs) and nonlocalized initial conditions (NLICs). The former is a bell-shaped function as shown in Fig. 1(a). The latter is a Gaussian-shaped function in one dimension and almost constant in the transverse direction [see Fig. 1(b)]. Periodic or no-flux boundary conditions lead to the same results asymptotically in time.

III. RESULTS AND DISCUSSION

Figure 2(a) presents the overview of our previous qualitative main results [37] found for dissipative solitons localized in two spatial dimensions using LICs. The phase diagram presents the stable localized solutions observed for a large range of the bifurcation parameter μ, which is varied from $\mu = -0.55$ to $\mu = -0.30$. On the ordinate we have plotted the cubic part of the nonlinear refractive index, which is the second parameter we varied. In this phase diagram we observe a total of five transitions, three of which have not been observed in one dimension. This pertains to all transitions involving azimuthally symmetric exploding dissipative solitons, which have no analog in one spatial dimension.

A rather interesting transition is clearly the one from azimuthally symmetric to asymmetric exploding solitons. The other types of localized solutions found are stable stationary pulses such as are known to exist stably for the cubic-quintic Ginzburg-Landau-equation in one and two spatial dimensions [10,15]. We also note that Fig. 2(a) contains a direct transition between collapse (all classes of bounded initial conditions including localized ones decay as a function of time) and azimuthally symmetric explosions.

In Fig. 2(b) we have plotted the analog of Fig. 2(a) for quasi-1D dissipative solitons using NLICs. We note that their range of stable existence includes that covered in Fig. 2(a) as a subset. This means that quasi-1D solutions cover a large range in parameter space and are rather robust in their existence. We also note that a breathing quasi-1D state intervenes at the transition from stationary quasi-1D solutions to collapse (amplitude-zero solutions). We would like to point out that Fig. 2(b) delineates the maximum range of stable breathing quasi-1D solutions and that at the boundaries of this regime frequently a coexistence with collapse or stationary quasi-1D solutions occurs for fixed parameter values, indicative of a small amount of hysteresis.

As we discussed, stable quasi-1D states exist over a large parameter regime. For example for $\beta_i = 0.75$ the range of stable existence includes $-1.1 \leqslant \mu \leqslant -0.0$. By stable we

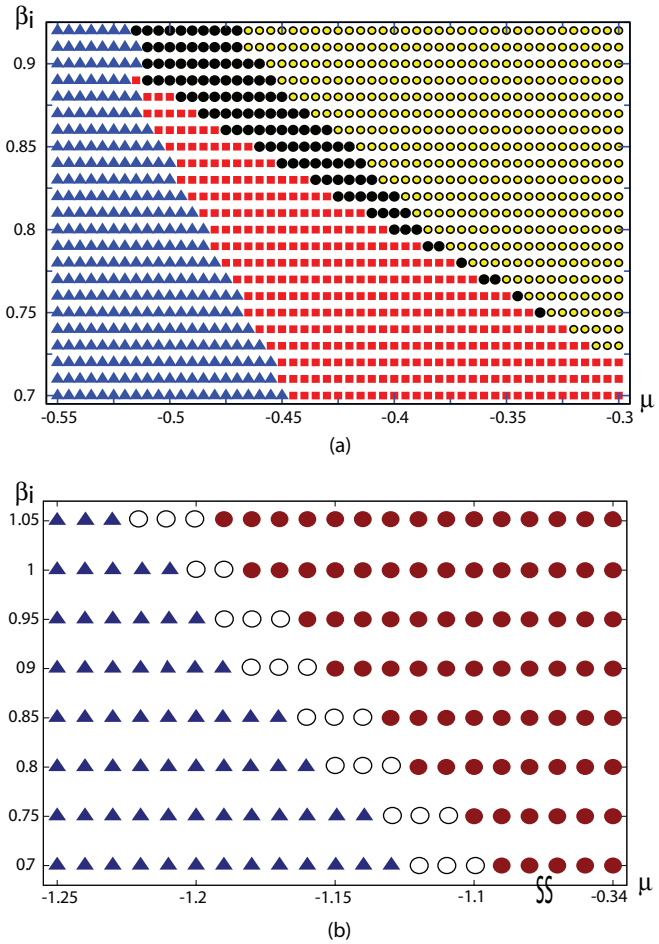

FIG. 2. (Color online) (a) Phase diagram, using numerical method I, showing the observed stable patterns as a function of the cubic nonlinear refractive index β_i on the ordinate versus the bifurcation parameter μ using LICs. We show the parameter range μ from -0.55 to -0.3. It includes (i) solutions with amplitude zero (solid triangles, ▲), (ii) stationary localized solutions (solid squares, ■), (iii) azimuthally symmetric exploding localized solutions shown as black solid circles (●), and asymmetric exploding localized solutions given by the open circles (○). All data points shown have been obtained with numerical runs with a duration $T = 5 \times 10^3$ corresponding to 5×10^5 iterations. We note that the boundaries between the different types of behavior shown are not completely sharp, but that any possible hysteresis is smaller than the size of the symbols used. (b) Phase diagram, using numerical method II, obtained using NLICs, showing the range of existence for quasi-1D solutions as red solid circles (●), breathing quasi-1D solutions as open circles (○), and collapse (amplitude zero) as blue solid triangles (▲). On the ordinate β_i covers the range $0.7 \leqslant \beta_i \leqslant 1.05$ while the parameter values for the bifurcation parameter μ are $-1.27 \leqslant \mu \leqslant -0.34$, where the regime $\mu \leqslant -1.00$ is presented in detail. The break indicates that the same behavior continues all the way up to $\mu = -0.34$. We note that the parameter range covered in plot (b) contains the parameter range presented in (a) essentially as a subset.

mean in this context stable against noisy perturbations, which are applied for a finite amount of time and then taken away again. Over this range one has other locally stable solutions

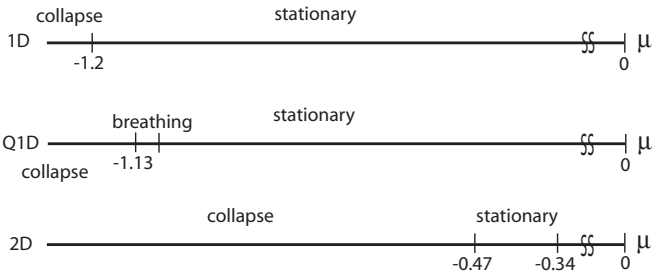

FIG. 3. We plot for fixed value of β_i, $\beta_i = 0.75$, the range of localized solutions of the 1D equation as well as the quasi-1D and the 2D localized solutions as a function of the bifurcation parameter μ for $-1.30 \leqslant \mu \leqslant 0$ using a linear scale. For quasi-1D localized solutions the break indicates that the same behavior continues all the way up to $\mu = 0$, while for localized solutions in 1D as well as for localized solutions in 2D the break indicates that other types of localized solutions occur above the break. For localized solutions in 2D this regime covers the range between $\mu = -0.34$ and $\mu = 0$. We note that the range of stable stationary radially symmetric solutions in 2D is contained as a subset in the bifurcation parameter range for stable 1D and quasi-1D stationary localized solutions.

with increasing μ: stationary localized solutions, azimuthally symmetric exploding localized solutions (over a very narrow parameter range), and asymmetric localized solutions. As we will show below 2D stationary localized solutions can combine with quasi-1D states to form a stable compound state.

For $\beta_i = 1.00$ the range of stable existence of quasi-1D solutions includes $-1.18 \leqslant \mu \leqslant -0.26$. Over this range one has other locally stable solutions with increasing μ: azimuthally symmetric exploding localized solutions and asymmetric exploding localized solutions. As we will show below 2D azimuthally symmetric exploding localized solutions can combine with quasi-1D states to form a stable compound state.

In Fig. 3 we have plotted for fixed β_i, $\beta_i = 0.75$, a comparison between one and two spatial dimensions. We note that the range of stable existence for the quasi-1D solutions is almost as large as that for the stationary pulse solutions found first by Thual and Fauve [10]. Only close to the left boundary is an instability possible for the stationary quasi-1D solutions, leading first to breathing quasi-1D solutions and then to collapse. We notice that for these parameter values the 1D equation does not have breathing solutions. The situation is rather different when the comparison is made for the localized solutions in 2D. Radially symmetric stationary solutions exist stably only for $-0.47 \leqslant \mu \leqslant -0.34$. For smaller values of the bifurcation parameter μ, the solutions localized in 2D collapse, while for larger values of μ the radially symmetric 2D solutions are replaced by a number of time-dependent and exploding solutions—compare Fig. 2(a).

In Fig. 4 we compare the profile of the amplitude $R(x,y) = |A((x,y)|$ for fixed values of the parameters β_i and μ for the stationary quasi-1D solution with that of the radially symmetric 2D stationary solution. It emerges that the 2D pulse has an amplitude which is about 25% less than that of the quasi-1D pulse, while its width is about 20% larger. We also emphasize that the profiles of the stationary pulse solutions of the 1D equation and of the quasi-1D solutions of the 2D equation are identical. This can be understood easily from the

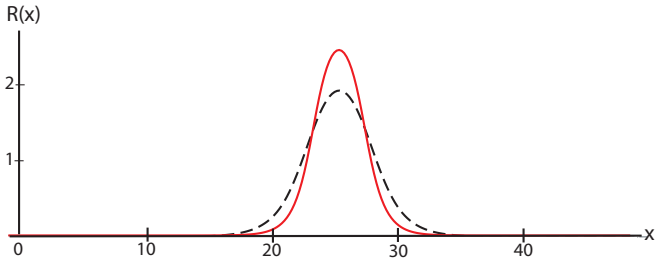

FIG. 4. (Color online) The amplitude profile $R(x,y) = |A(x,y)|$ plotted as a function of x for the quasi-1D (solid line) and the radially symmetric 2D solutions (dashed line) for fixed values of β_i ($\beta_i = 0.75$) and the bifurcation parameter μ ($\mu = -0.40$). One clearly sees a reduction in amplitude for the radially symmetric 2D solution by about ∼25%, while its width (FWHM) is ∼20% larger when compared to the quasi-1D solution. We note that the profiles for the stationary 1D solution of the 1D equation and of the quasi-1D solutions of the 2D equation are identical.

fact that for the stationary quasi-1D solutions the derivatives in the second direction (along the crest of the quasi-1D solutions) are zero.

It also emerges that for all parameter values for which we have investigated the simultaneous stable existence of quasi-1D solutions and 2D asymmetric exploding localized solutions their interaction always led to the destruction of the 2D asymmetric exploding localized solutions, with the quasi-1D solutions left over indefinitely.

In Fig. 5 (Fig. 6) we have plotted the amplitude $R(x,y,t) = |A(x,y,t)|$ for eight different times between symmetric (asymmetric) explosions, respectively [39]. We remark that the time between explosions is not fixed but that it is given by a narrow distribution. We note that in particular the large-amplitude behavior during the explosions is qualitatively different in the two cases. We also emphasize that the large-amplitude behavior for the spatiotemporal patterns associated with

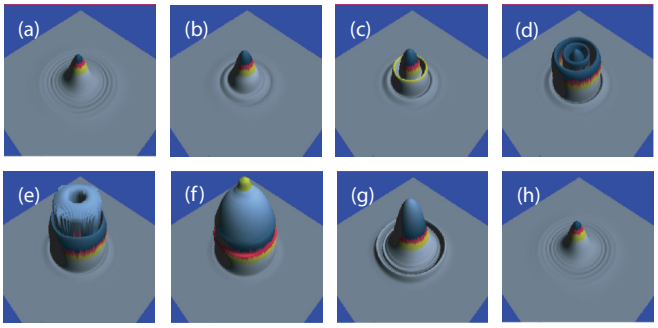

FIG. 5. (Color online) (a) $T = 0$, (d) $T = 17.6$, (f) $T = 18.4$, (h) $T = 31$. Eight snapshots of $|A(x,y,t)|$ are plotted characteristic of the time evolution of an azimuthally symmetric exploding dissipative soliton The parameters chosen for these snapshots are $\mu = -0.5$ and $\beta_i = 1.0$. All other parameter values are the same as given in the text. Snapshots (d) to (f) in the sequence show the vicinity of the explosions, demonstrating clearly the qualitative difference between azimuthally symmetric and asymmetric explosions. The amplitude increases by about 50% during the explosion. Note that the azimuthal symmetry is completely preserved during the explosion. The duration of the explosion is about 3% of the time between explosions.

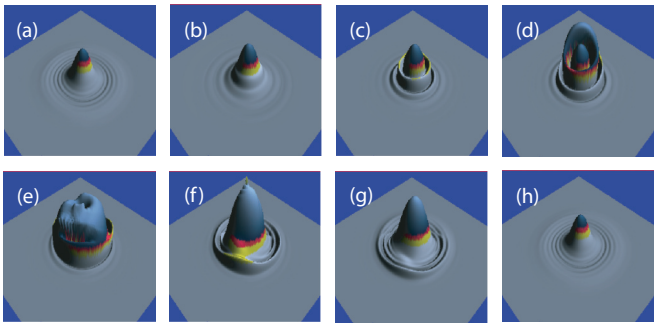

FIG. 6. (Color online) (a) $T = 0$, (d) $T = 11$, (f) $T = 13.5$, (h) $T = 15.8$. Eight snapshots of $|A(x,y,t)|$ are plotted characteristic of the time evolution of an asymmetric dissipative soliton. The parameters chosen for these snapshots are $\mu = -0.3$ and $\beta_i = 1.0$. All other parameter values are the same as given in the text. Snapshots (d) to (f) in the sequence show the vicinity of the explosions, demonstrating clearly the qualitative difference between azimuthally symmetric and asymmetric explosions. The duration of the explosion is about 15% of the time between explosions. The amplitude increases by about 50% during the explosion.

asymmetric explosions is never repeated precisely from one explosion to the next because of its chaotic nature.

In Fig. 7 we show a stable quasi-1D solution for $\mu = -0.5$ and $\beta_i = 1.0$ and in Fig. 8 a snapshot of a stable breathing quasi-1D solution for $\mu = -1.24$ and $\beta_i = 1.05$. In this case it is also important to stress that the cross sections in the plane spanned by the amplitude $R(x,y,t)$ and the x direction are breathing as shown in the x-t plot in Fig. 9 as a function of time as well (compare Ref. [16] for breathing localized solutions in 1D). We are not aware of any report of such a breathing quasi-1D solution in any other system, but speculate that it will intervene typically near the boundary between stationary quasi-1D solutions and collapse. It will therefore be very worthwhile to investigate the analogs of these solutions for other systems like optical systems with a saturation nonlinearity including optical bistability and a laser with a saturable absorber [1,19] and the cubic-quintic Swift-Hohenberg equations [2,24].

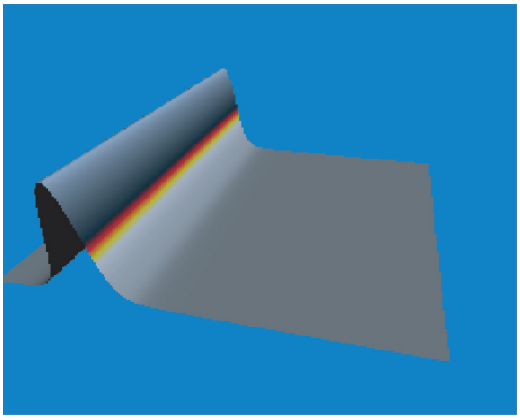

FIG. 7. (Color online) The magnitude of the amplitude $|A(x,y,t)|$ for a quasi-1D state for $\mu = -0.5$ and $\beta_i = 1.0$; all other parameter values are the same as given in the text.

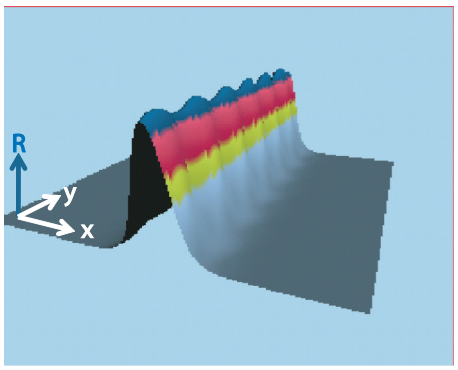

FIG. 8. (Color online) Snapshot of the magnitude of the amplitude $|A(x,y,t)|$ for a breathing quasi-1D state for $\mu = -1.24$ and $\beta_i = 1.05$ as it arises near the quasi-1D to collapse transition in the form of a standing oscillation. All other parameter values are the same as given in the text.

We note that the symmetry in the case of the quasi-1D solutions is already broken due to the initial conditions from which they are obtained: the generic nonlocalized initial conditions shown in Fig. 1(b). For example, a different direction initially for the NLICs will lead to a different direction of the quasi-1D solution as well. This is thus also a feature similar to the corresponding objects studied in Refs. [6,7].

To study the nature of the transition from stable quasi-1D solutions to stable breathing quasi-1D solutions we fixed $\beta_i = 0.8$, varied μ, and measured $R(x = \frac{L}{2}, y = 0, t; \mu) = |A(x = \frac{L}{2}, y = 0, t; \mu)|$, where $L \times L$ is the box size. We used generic nonlocalized initial conditions as shown in Fig. 1(b) and performed up to 10^8 iterations to avoid transients. The result is that beyond a critical value μ_c the amplitude $R(x = \frac{L}{2}, y = 0, t; \mu)$ undergoes an oscillatory instability, in this case, a forward Hopf bifurcation. Thus, close to the instability, the amplitude $R(x = \frac{L}{2}, y = 0, t; \mu)$ takes the form

$$R\left(x = \frac{L}{2}, y = 0, t; \mu\right) = R_{st}(\mu) + \xi(t) + \text{c.c.}, \qquad (3)$$

where $R_{st}(\mu)$ is the value of the amplitude of the stable quasi-1D solution at $x = \frac{L}{2}$ and $y = 0$. The complex field $\xi(t)$ can be

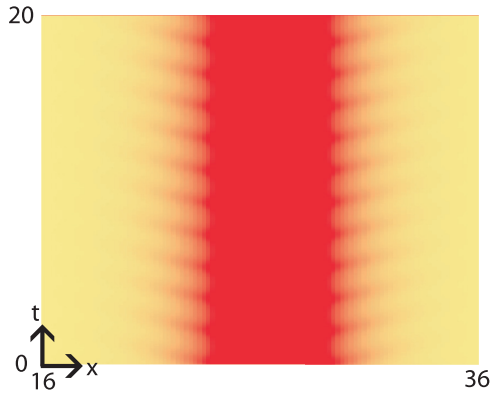

FIG. 9. (Color online) An x-t plot of a cross section spanned by $R(x,y,t)$ and the x direction of the quasi-1D solution shown in Fig. 8.

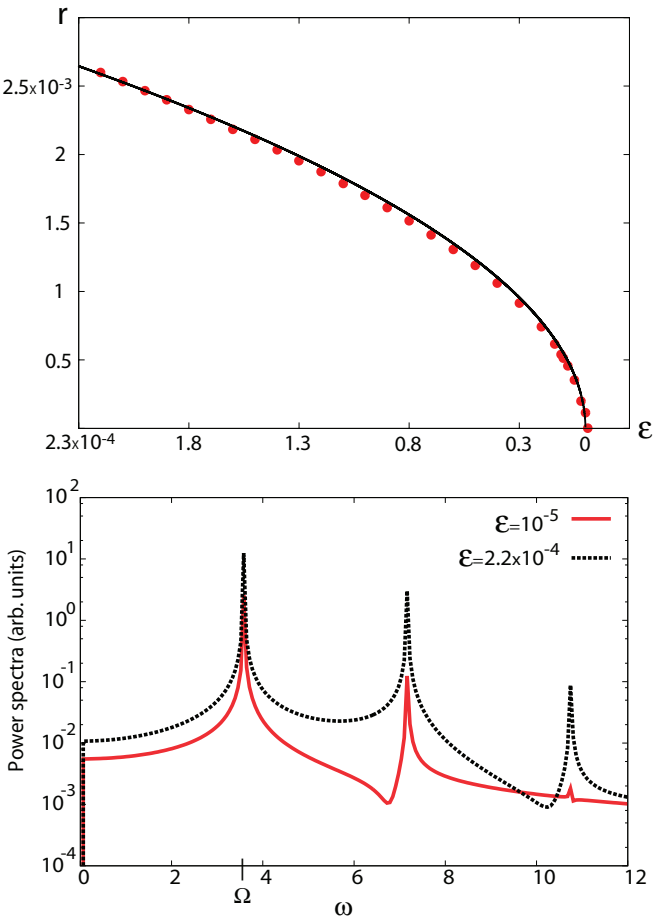

FIG. 10. (Color online) (a) $r = 2|\xi(t \to \infty)|$ plotted as a function of $\varepsilon \equiv \mu_c - \mu$, resulting in $\mu_c = -1.123\,47$ and $r = r_0\sqrt{\varepsilon}$, where $r_0 = 0.1744$. (b) Power spectra of $R(x = L/2, y = 0, t; \mu)$ for two different values of ε, namely, $\varepsilon = 10^{-5}$ and $\varepsilon = 2.2 \times 10^{-4}$. The spectra show that the values of the main frequencies ($\Omega = 3.58$) and harmonics are not sensitive to ε (or μ).

described by the normal form for a forward Hopf bifurcation

$$\xi_t = (\varepsilon + i\Omega)\xi - (b_r + ib_i)|\xi|^2\xi, \qquad (4)$$

where $\varepsilon \equiv \mu_c - \mu$, and Ω is the main frequency as shown in Fig. 10(b). Since the main frequency seems to be independent of μ the nonlinear dispersion b_i must vanish while $b_r = \frac{4}{r_0^2}$. In Fig. 10(a) we plotted $r = 2|\xi(t \to \infty)|$ as a function of ε, and we find $r = r_0\sqrt{\varepsilon}$. In addition we checked that the main frequency Ω is rather insensitive to variations of β_i. In Fig. 9 we show an x-t plot of a cross section of the quasi-1D solution shown in Fig. 8. The breathing shows a period of 1.81, equivalent to a main frequency of 3.46 for $\beta_i = 1.05$.

In the course of our investigations we have found two types of stable compound states involving stationary quasi-1D solutions. In Fig. 11 we have plotted a compound object composed of a quasi-1D solution and a 2D stationary localized solution. The parameter values are $\beta_i = 0.75$ and $\mu = -0.40$. Close inspection of the compound state reveals that the quasi-1D part of this compound state is emitting waves which are damped out in the wings of the 2D stationary localized

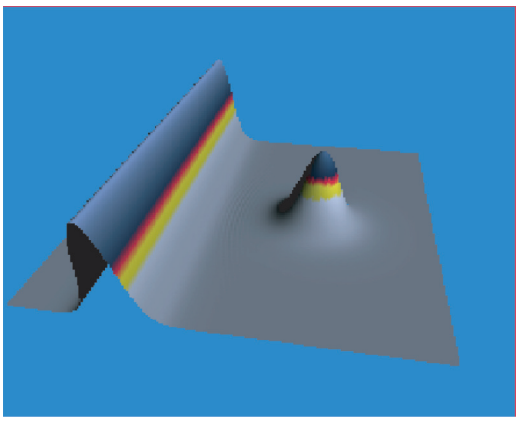

FIG. 11. (Color online) $|A(x,y,t)|$ for a snapshot of a compound state of a quasi-1D solution and a radially symmetric 2D stationary dissipative soliton for $\mu = -0.4$ and $\beta_i = 0.75$. All other parameter values are the same as given in the text.

solution. This is clearly brought out in the magnified view shown in Fig. 13(a).

In Fig. 12 we have plotted a compound object composed of a quasi-1D solution and an azimuthally symmetric exploding localized solution. The parameter values are $\beta_i = 1.00$ and $\mu = -0.50$. Note that we have shown in Fig. 5 for comparison eight snapshots in the time evolution of an azimuthally symmetric exploding localized solution for the same parameter values. Close inspection of the compound state reveals that both parts of this compound state are emitting waves of different wavelengths and different frequencies with a wave amplitude of about 0.6% of the maximum amplitude of the compound state. This is shown magnified in Fig. 13(b). We also note that these emitted waves lead to a line which acts as a sink due to the presence of the waves coming down from the azimuthally symmetric exploding dissipative soliton as well.

From these two observations the following picture emerges. Waves are emitted in both cases by the quasi-1D states to adjust to curvature effects imposed by the 2D stationary

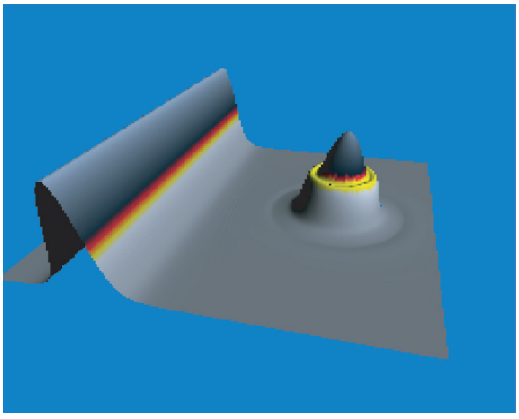

FIG. 12. (Color online) $|A(x,y,t)|$ for a snapshot of a compound state of a quasi-1D solution and an almost azimuthally symmetric exploding dissipative soliton for $\mu = -0.5$ and $\beta_i = 1.0$. Note that due to the interaction there is a preferred direction now, so that the azimuthal symmetry is broken in the presence of the quasi-1D state. All other parameter values are the same as given in the text.

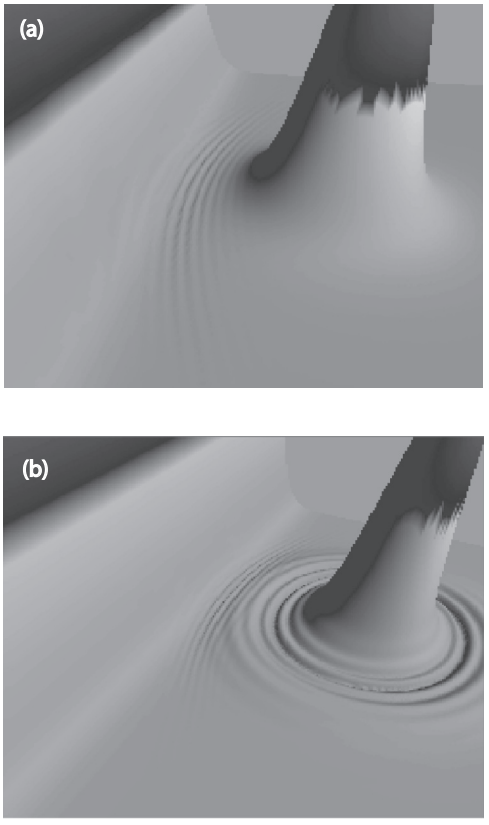

FIG. 13. The small-amplitude behavior in the stable compound states in between the quasi-1D state and the 2D stationary localized state (a) and the azimuthally symmetric exploding dissipative soliton (b) plotted in the asymptotic time regime. Both parts are shedding waves of a different wavelength and different frequency in (b), leading to a line sink, while in (a) only the quasi-1D part of the compound state is emitting waves, which are damped out in the wings of the 2D localized solution. The parameters are $\mu = -0.4$ and $\beta_i = 0.75$ for (a) and $\mu = -0.5$ and $\beta_i = 1.0$ for (b). All other parameter values are the same as given in the text.

localized solution and by the azimuthally symmetric exploding localized solution, respectively. Clearly an isolated stationary quasi-1D state does not shed any waves, thus demonstrating the interaction with the localized states in 2D that are close by.

If one has initially two quasi-1D states sufficiently far apart, their final state shows no dynamics and they just coexist indefinitely. Furthermore, we find that if one has in the beginning two quasi-1D states sufficiently close to each other, they combine and form one stationary quasi-1D state, which has the same universal width as all quasi-1D states for fixed parameter values, which is effectively indicative of a partial annihilation [29].

Figures 11 to 13 raise the issue of an optimal distance between stationary or azimuthally symmetric exploding dissipative solitons and the quasi-1D solution. In this connection we would like to state the following: If the distance between the quasi-1D solution and the stationary or azimuthally symmetric exploding solution is too small, the quasi-1D solution absorbs the other type of solution. Thus there is clearly a minimum distance over which we can observe the behavior shown in the

blowups in Fig. 13. If, however, the distance is very large, the interaction between the two objects becomes negligible.

Finally we would like to point out that we have never observed a compound state formed by a quasi-1D state and a 2D asymmetric exploding solution. Instead, asymptotically in time, the 2D asymmetric exploding localized solution was always annihilated by the quasi-1D solution. This result can be traced back to the fact that 2D asymmetric exploding localized solutions show a mean motion of their center of mass [37] and thus collide dynamically with the static quasi-1D solutions. This situation has to be contrasted with the case of the 2D azimuthally symmetric exploding localized solution, which shows almost no mean center of mass motion—except for that induced by the presence of the stationary quasi-1D state, which leads by its very presence to a preferred direction. As has been argued in [37], the center of mass of asymmetric explosive solitons exhibits a random walk.

IV. PERSPECTIVE

From the results described above, clearly several different directions emerge where one can generalize and/or apply the present analysis. We expect the occurrence of—as well as the transition to—breathing quasi-1D localized states also for other prototype equations, including Swift-Hohenberg equations and equations with saturation-type nonlinearity, as they arise naturally in nonlinear optics.

On the experimental side it is certainly very desirable to compare in more detail the properties of the quasi-1D states investigated here with those found experimentally in a convective system with local heating by Miranda and Burguete [6,7]. Naturally one can also ask the question for which other experimentally accessible systems one could realize quasi-1D states of the type discussed in the present paper. Clearly the systems that come to mind first are from nonlinear optics since they have become very versatile with respect to the investigation of the influence of spatial degrees of freedom on pattern formation over the last decade or so [23,40].

ACKNOWLEDGMENTS

We thank Carlos Cartes for helping us with the calculations leading to Fig. 10. O.D. wishes to acknowledge the support of FONDECYT (Project No. 1110360) and Universidad de los Andes through FAI initiatives. H.R.B. thanks the Deutsche Forschungsgemeinschaft for partial support of this work through the Forschergruppe FOR 608, "Nichtlineare Dynamik komplexer Kontinua."

[1] H. R. Brand and R. J. Deissler, Physica A **204**, 87 (1994).
[2] H. Sakaguchi and H. R. Brand, Physica D **97**, 274 (1996).
[3] H. Sakaguchi and B. A. Malomed, Physica D **159**, 91 (2001).
[4] H. Sakaguchi and B. A. Malomed, Physica D **167**, 123 (2002).
[5] J. Burke and E. Knobloch, Chaos **17**, 102 (2007).
[6] M. A. Miranda and J. Burguete, Phys. Rev. E **78**, 046305 (2008).
[7] M. A. Miranda and J. Burguete, Phys. Rev. E **79**, 046201 (2009).
[8] J. M. Soto-Crespo, N. Akhmediev, and A. Ankiewicz, Phys. Rev. Lett. **85**, 2937 (2000).
[9] S. T. Cundiff, J. M. Soto-Crespo, and N. Akhmediev, Phys. Rev. Lett. **88**, 073903 (2002).
[10] O. Thual and S. Fauve, J. Phys. (France) **49**, 1829 (1988).
[11] H. R. Brand and R. J. Deissler, Phys. Rev. Lett. **63**, 2801 (1989).
[12] P. Kolodner, Phys. Rev. A **44**, 6448 (1991).
[13] P. Kolodner, Phys. Rev. A **44**, 6466 (1991).
[14] H. H. Rotermund, S. Jakubith, A. von Oertzen, and G. Ertl, Phys. Rev. Lett. **66**, 3083 (1991).
[15] R. J. Deissler and H. R. Brand, Phys. Rev. A **44**, 3411 (1991).
[16] R. J. Deissler and H. R. Brand, Phys. Rev. Lett. **72**, 478 (1994).
[17] R. J. Deissler and H. R. Brand, Phys. Rev. E **51**, 852 (1995).
[18] R. J. Deissler and H. R. Brand, Phys. Rev. Lett. **74**, 4847 (1995).
[19] H. R. Brand and R. J. Deissler, Physica A **216**, 288 (1995).
[20] P. B. Umbanhowar, F. Melo, and H. L. Swinney, Nature (London) **382**, 793 (1996).
[21] V. V. Afanasjev, N. Akhmediev, and J. M. Soto-Crespo, Phys. Rev. E **53**, 1931 (1996).
[22] T. Ohta, Y. Hayase, and R. Kobayashi, Phys. Rev. E **54**, 6074 (1996).
[23] V. B. Taranenko, K. Staliunas, and C. O. Weiss, Phys. Rev. A **56**, 1582 (1997).
[24] H. Sakaguchi and H. R. Brand, Physica D **117**, 95 (1998).
[25] O. Lioubashevski, Y. Hamiel, A. Agnon, Z. Reches, and J. Fineberg, Phys. Rev. Lett. **83**, 3190 (1999).
[26] E. A. Ultanir, G. I. Stegeman, D. Michaelis, C. H. Lange, and F. Lederer, Phys. Rev. Lett. **90**, 253903 (2003).
[27] P. Tsai, S. W. Morris, and Z. A. Daya, Europhys. Lett. **84**, 14003 (2008).
[28] A. Ankiewicz, N. Devine, N. Akhmediev, and J. M. Soto-Crespo, Phys. Rev. A **77**, 033840 (2008).
[29] O. Descalzi, J. Cisternas, D. Escaff, and H. R. Brand, Phys. Rev. Lett. **102**, 188302 (2009).
[30] A. C. Newell, *Solitons in Mathematics and Physics* (SIAM, Philadelphia, 1985).
[31] N. Akhmediev, J. M. Soto-Crespo, and G. Town, Phys. Rev. E **63**, 056602 (2001).
[32] N. Akhmediev and J. M. Soto-Crespo, Phys. Lett. A **317**, 287 (2003).
[33] N. Akhmediev and J. M. Soto-Crespo, Phys. Rev. E **70**, 036613 (2004).
[34] O. Descalzi and H. R. Brand, Phys. Rev. E **82**, 026203 (2010).
[35] O. Descalzi, C. Cartes, J. Cisternas, and H. R. Brand, Phys. Rev. E **83**, 056214 (2011).
[36] C. Cartes, O. Descalzi, and H. R. Brand, Phys. Rev. E **85**, 015205 (2012).
[37] C. Cartes, J. Cisternas, O. Descalzi, and H. R. Brand, Phys. Rev. Lett. **109**, 178303 (2012).
[38] A. Kloeckner, N. Pinto, Y. Lee, B. Catanzaro, P. Ivanov, and A. Fasih, Parallel Comput. **38**, 157 (2012).
[39] The color has been chosen to give both online (color) and in print (gray scale) a plastic and intuitive picture of the time evolution and the various spatial features of the different types of localized solutions in three dimensions shown in Figs. 5–8, 11, and 12.
[40] P. Genevet, S. Barland, M. Giudici, and J. R. Tredicce, Phys. Rev. A **79**, 033819 (2009).